nature communications

Article

https://doi.org/10.1038/s41467-026-72648-6

Evidence of hydrological regime shifts associated with a major decades-long drought in West Africa

Received: 16 July 2025

Accepted: 20 April 2026

Published online: 07 May 2026

Check for updates

Christophe Peugeot[1], Valentin Wendling[2], Erwan Le Roux[3], Gérémy Panthou[4], Basile Hector[4], Nathalie Rouché[1], Arthur Crespin-Boucaud[1], Guillaume Favreau[4], Farida Boubé Dobi[4,5], Jean-Martial Cohard[4], Jerôme Demarty[1], Luc Descroix[6], Jordi Etchanchu[1], Manuela Grippa[7], Pierre Hiernaux[8], Aghali Ingatan Warzagan[9], Laurent Kergoat[7], Moussa Malam Abdou[10], Eric Mougin[7], Caroline Pierre[11], Jean-Louis Rajot[11], Jean-Pierre Vandervaere[4], Théo Vischel[4] & Thierry Lebel[4]

Using ground-based meteorological, hydrological and land cover datasets from 1950 to 2015, we provide evidence that the increase in runoff observed in the semi-arid central Sahel (West Africa) since the 1970-1995 drought is a shift between alternative stable states of low and high runoff. We propose a conceptual model, governed by feedback loops between vegetation and surface runoff, which describes the stabilising mechanisms of each state and the basin-scale impact of local shifts. While the drought was likely the trigger for the shift, land clearing and rainfall intensification may have reinforced it. Due to wetter conditions and greater resilience, other basins further south did not shift. Our study suggests that the shift towards higher runoff is due to surface processes playing a dominant role in this region, with minimal contribution from subsurface processes. This regime shift framework offers a promising perspective on understanding long-term hydrological changes.

According to the system dynamics theory, a regime shift is a significant change in the way a complex system operates, resulting in a transition between alternative states[1]. Each state corresponds to a particular way of functioning, or 'regime', of the system. These states are usually associated with feedback loops that stabilise the system. If a disturbance in the forcing factors is sufficiently strong, it can drive the system beyond a critical threshold (a 'tipping point'), triggering a transition to an alternative state. The system is then trapped in the new state even if the disturbance ceases, with little or no reversibility, with respect to the characteristic timescales of the triggering factors. The concept of multiple stable states and regime shifts in environmental systems was advocated as early as the 1970s[2], and has since been applied to various topics[3–6] including social-ecological systems[7].

When exposed to rainfall deficits, watersheds may typically exhibit such non-linear responses[8–10]. Recent studies in Australia and North America have shown that watersheds affected by multi-year droughts may have permanently shifted towards lower annual streamflow for a given annual rainfall, even under wetter post-drought conditions[11,12].

[1]HSM, IRD, Université de Montpellier, CNRS, Montpellier, France. [2]HSM, Université de Montpellier, IMT Mines Alès, CNRS, IRD, Alès, France. [3]Lab-STICC, UMR CNRS 6285, IMT Atlantique, Brest, France. [4]IGE, Université Grenoble Alpes, Grenoble INP, INRAE, CNRS, IRD, Grenoble, France. [5]Département de Géologie, Faculté des Sciences et Techniques, Université Abdou Moumouni, Niamey, Niger. [6]PALOC, IRD, MNHN, CNRS, Paris, France. [7]GET, Université de Toulouse, CNRS, IRD, CNES, Toulouse, France. [8]PASTOC, Caylus, France. [9]Département de Géographie, Université Abdou Moumouni, Niamey, Niger. [10]Département de Géographie, Université André Salifou, Zinder, Niger. [11]IEES, Sorbonne Université, Université Paris Cité, Université Paris Est Créteil, CNRS, IRD, INRAE, Paris, France. e-mail: christophe.peugeot@ird.fr

https://doi.org/10.1038/s41467-026-72648-6

Long-lasting hydrological changes have also been documented in West Africa[13–15]. This makes it an ideal case study for further exploration of hydrological regime shifts. The West African Sahel and its neighbouring regions—the Sahara to the north and the Sudanian area to the south—experienced a regional drought between 1970 and the mid-1990s. Annual rainfall deficits of about 150 to 200 mm were observed, corresponding to a relative deficit of about 50% in the north of the region and about 10% in the south[16]. The drought occurred alongside significant human-induced land clearing, which began in the 1940s and intensified due to population growth and an increased demand for food and fuel wood. As a result, a 37% reduction in natural vegetation cover was observed in the Sahel and a 54% reduction in the Sudanian area between 1975 and 2000[17]. This drought ended in the mid-1990s, but it did not lead to a recovery of pre-drought conditions, as annual rainfall remained below pre-drought levels, and rainfall intensity increased as a result of fewer but larger events[18]. In the Sudanian region, basin-scale observations show a decrease in runoff during the drought, followed by an increase, which is consistent with changes in precipitation. In contrast, in the central Sahel, runoff has paradoxically increased by 40–60% since the onset of the drought[13–15]. This counterintuitive behaviour—the so-called 'Sahelian paradox', Descroix et al.[13]—has been attributed to the effect of land clearing on runoff, which has largely outweighed the effect of the rainfall deficit[19–23]. However, in the northern Sahel, rain-fed agriculture is rare, and the increase in runoff has been attributed to drought-induced vegetation dieback and associated land degradation rather than to human impact[24–26]. Since the end of the 1980s, regreening of herbaceous and tree cover has been reported in most parts of the Sahel[27–29], thanks to both larger annual rainfall and elevated atmospheric CO_2 concentrations[30]. Since runoff is generally expected to decrease with vegetation growth, this could indicate another paradoxical behaviour. Combined with the other unexpected changes observed, this could suggest an underlying regime shift.

Hydrological regime shifts have multiple implications for water resources[31], hydrological risk mitigation and adaptation strategies, particularly in this region. For example, local communities and stakeholders may wish to know whether the new opportunities offered by increased runoff and additional water resources will persist, as e.g. in South-West Niger[32,33]. A shift to the high runoff state implies that the recurrent devastating floods observed since the 2010s[34,35] could persist regardless of how the rainfall regime evolves. Regime shifts could also inform land restoration and sustainable water resource management initiatives by taking advantage of self-reinforcing feedback processes[36–38]. More broadly, hydrological shifts associated with land surface changes may be local components of larger-scale surface-atmosphere feedback loops that impact the regional or global climate by altering soil moisture and the way in which the land surface responds to atmospheric conditions[39].

In this study, we propose that the West African basins have alternative states – or regimes—of low and high runoff, which are maintained by feedback loops between water, soil and vegetation (the RS hypothesis hereafter). Accordingly, hydrological changes may reflect a shift between these two states, triggered by perturbations such as drought or anthropogenic land cover changes. Previous work at the hillslope scale[40] showed the relevance of the regime shift concept for interpreting the degradation of a Sahelian ecosystem as a transition from a vegetated state to a bare soil state, triggered by drought. However, no general conclusions about regional hydrology could be drawn from this single local case. Here we focus on a series of sub-Saharan basins ranging from 7000 to 50,000 km^2 and spanning the regional hydroclimatic gradient (Fig. 1). We used a unique 65-year dataset of ground-based meteorological, hydrological and land cover observations over the period 1950–2015. Long periods of observation are needed to evidence regime shifts, in order to cancel out any delayed or transient response to perturbations. The paper has two objectives: (i) to demonstrate that the observed hydrological changes in the Sahel correspond to a regime shift; and (ii) to propose a conceptual model based on feedback mechanisms to explain why and how this shift occurred.

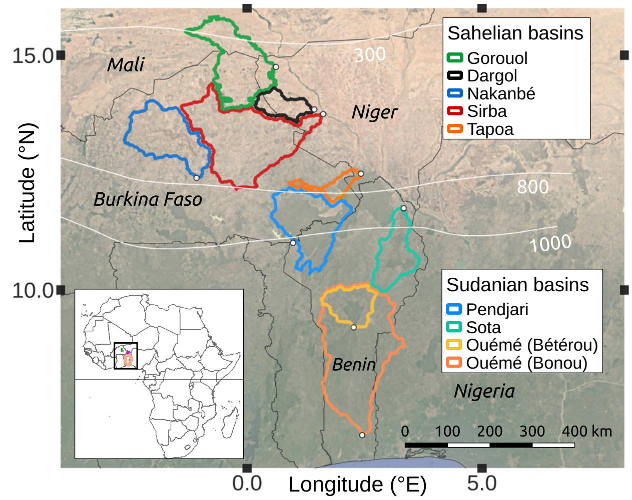

Fig. 1 | Basins location and the 300-, 800- and 1000-mm isohyets are shown as white lines. The Sahelian and Sudanian basins lie north and south of the 800-mm isohyet, respectively. Background image from Google Earth (Google, Landsat/Copernicus, Data SIO, NOAA, U.S. Navy, GEBCO, Map Data © 2026 AND), and country borders from OpenStreetMap (ODbL license).

We provide evidence that the increase in runoff observed in the semi-arid central Sahel (West Africa) since the severe regional 1970–1995 drought is a shift between alternative stable states of low and high runoff. We found no equivalent regime shift towards higher runoff after a drought in recent literature. We propose a conceptual model governed by feedback loops between vegetation, soil properties, and surface runoff, which provides a coherent framework through which to describe the stabilising and destabilising mechanisms of each state. This model is consistent with the observations of multiple localised shifts affecting only parts of the landscape, leading to basin-scale shifts. The severe aridity conditions of the drought were likely the trigger of the shift, although anthropogenic land clearing and rainfall intensification may have played a reinforcing role. In contrast, the absence of a shift in the wetter Sudanian basins is likely due to less severe drought conditions and greater resilience. Our results suggest that the unexpected increase in runoff for the same annual rainfall reported here—opposite to regime shifts documented on other continents—is due to dominant land surface processes driven by feedback mechanisms, with minimal contribution of underground processes.

Results

The ten sub-Saharan basins selected (Fig. 1) have the longest runoff records, spanning the period 1950–2015 (See 'Methods'). They are located in a region where significant research efforts have been deployed in recent decades[41–43]. The geological substratum of these basins consists of crystalline rocks from the African Precambrian Shield[44]. A saprolite layer 10–30 m thick overlays the fractured bedrock[45,46]. In the Sahelian area, detrital and aeolian sand deposits lie on top of the saprolite and thin to the south until they disappear in the Sudanian area. Groundwater systems are present throughout the region within the fractured bedrock and the overlying material. These systems are recharged annually by either focused or diffuse recharge, depending on the area[47]. The slopes are mostly gentle (less than 5%), and the altitude ranges from 250 to 400 m amsl inland from the Guinean coast. A few low mountain ranges reach 600 m amsl in the Ouémé basin (Fig. 1). The Sahelian basins are mainly occupied by mixed annual grass and tree savannahs or steppes and the Sudanian basins by

 https://doi.org/10.1038/s41467-026-72648-6

Table 1 | Basin characteristics: basin name (identical to the river name), outlet name and coordinates, countries in which the basin extends, surface area, type of climate, mean annual rainfall (1950–2015), typical extent of the rainy season and the streamflow period, and period over which streamflow data are available

Basin: River (Outlet, Lat; Lon)	Countries	Area (km^2)	Climate type	Annual rainfall (mm)	Rainy season	Streamflow period	Streamflow time series
Gorouol (Alcongui, 14.75N; 0.61E)	Mali, Burkina Faso, Niger	23,250	Sahelian	410	Jun–Sep	Jul–Sep	1961–2015
Dargol (Kakassi, 13.84N; 1.43E)	Burkina Faso, Niger	7350	Sahelian	500	Jun–Sep	Jul–Sep	1957–2015
Sirba (Garbe-Kourou, 13.74N; 1.62E)	Burkina Faso, Niger	40,290	Sahelian	600	May–Oct	Jun–Oct	1956–2015 (*)
Nakanbé (Wayen,12.38N; 1.08W)	Burkina Faso	21,180	Sahelian	660	May–Oct	Jun–Oct	1965–2014
Tapoa (W Camp, 12.47N; 2.42E)	Burkina Faso, Niger	5700	Sahelian	770	Apr–Oct	Jun–Oct	1963–2015
Pendjari (Porga, 10.99N; 0.98E)	Burkina Faso, Benin	23,740	Sudanian	930	Apr–Oct	Jul–Nov	1952–2006
Sota (Couberi, 11.73N; 3.33E)	Benin	13,500	Sudanian	1020	Mar–Oct	Jul–Nov	1953–2012
Ouémé (Bétérou, 9.20N; 2.27E)	Benin	10,280	Sudanian	1150	Mar–Oct	Jul–Dec	1952–2015 (*)
Ouémé (Bonou, 6.90N; 2.45E)	Benin, Nigeria	47,000	Sudanian	1180	Mar–Nov	Jun–Dec	1950–2014

(*) Extended dataset available, see Fig. S4.

mosaics of crops, perennial grass savannahs and woodlands. The basins are predominantly rural, with rain-fed agriculture. Most farming work is carried out by hand or with animal traction. Irrigation systems are not well developed[48,49], and groundwater pumping is primarily used for domestic water supply. Streamflow is intermittent throughout the region due to the seasonal nature of rainfall associated with the West African monsoon, except in the Great Niger and Volta rivers. The rainy season lasts 4–10 months, and the streamflow period 3–6 months depending on the basins (Table 1).

Eco-hydrological changes

Three sub-periods were identified in the annual rainfall series since 1950 (see 'Methods'): a wet period until 1969 (the pre-drought period), a drought period between 1970 and 1994, and a post-drought period from 1995 onwards, with wetter conditions than during the drought. The drought was defined by anomalies in annual rainfall amounts. Due to limitations in data availability, the common study period for all basins ends in 2015. For two basins, the rainfall and runoff datasets could be extended up to the 2020s (see 'Methods').

The rainfall anomaly as represented by the Standard Precipitation Index (*SPI*, see 'Methods') was fairly similar across all basins (Fig. 2a, b). All of them experienced the drought characterised by a first dry episode in 1973, and a paroxysm in 1984. The decadal variability is consistent with the regional trend[16], with more pronounced positive and negative anomalies in the north of the area. In the wetter period from the mid-1990s onwards, the anomalies became very similar with no obvious latitudinal effect.

The hydrological response of the basins to this drought disturbance, as described by the dimensionless annual runoff ratio K (see 'Methods'), greatly differed depending on the location. In the Sahelian basins, K increased since the onset of drought (Fig. 2c), whereas in the Sudanian basins, K decreased during the drought and then increased consistently with the rainfall signal (Fig. 2d).

Drastic changes in land cover have been documented in the region since the beginning of the satellite era in the mid-1970s[17]. To analyse these changes over a comparable period to the hydroclimatic data, we created additional land cover maps of the study basins dating back to the 1950s (see 'Methods'). This series provides four snapshots covering a period of 65 years, which is unprecedented for this region (Fig. 3). The land cover categories describe the type of land occupation, irrespective of land use (e.g. type of crops). Only the three dominant categories are shown. The 'woodland and savannah' category comprises areas with the highest level of tree cover compared to the other two categories. This category is not spatially homogeneous. It is dominated by woodlands and tree savannahs in the south, and by increasingly open grass and bush savannahs towards the north. The 'cropland' category refers to the landscape fraction dedicated to agriculture, resulting from shifting cultivation with periodic fallows and fields where woody plants are maintained. Fallows and savannahs are grazed by cattle.

Figure 3 shows a general decrease in woodlands or savannahs in all basins between 1950 and 2013, and an increase in cropland and, in some areas, bare soil. The decrease in the fraction of woodlands and savannahs indicates landscape opening and the impact of human activity. However, this does not imply a decrease in tree or grass density and is therefore not contradictory to regreening, which involves recovering herbaceous cover and increasing woody cover within land cover categories[29]. No systematic pattern emerges from north to south in the 'woodland and savannah' category, which decreases in all basins (Fig. 3). The greatest relative reduction in this category (41%) was observed in the Dargol basin (Table S1) and the lowest (10%) in the Pendjari basin, which partly extends over a protected nature reserve. In the other basins, the relative decrease in woodland and savannah amounted to roughly 20–30%. The main difference between the basins is the increase in bare soil areas since 1975

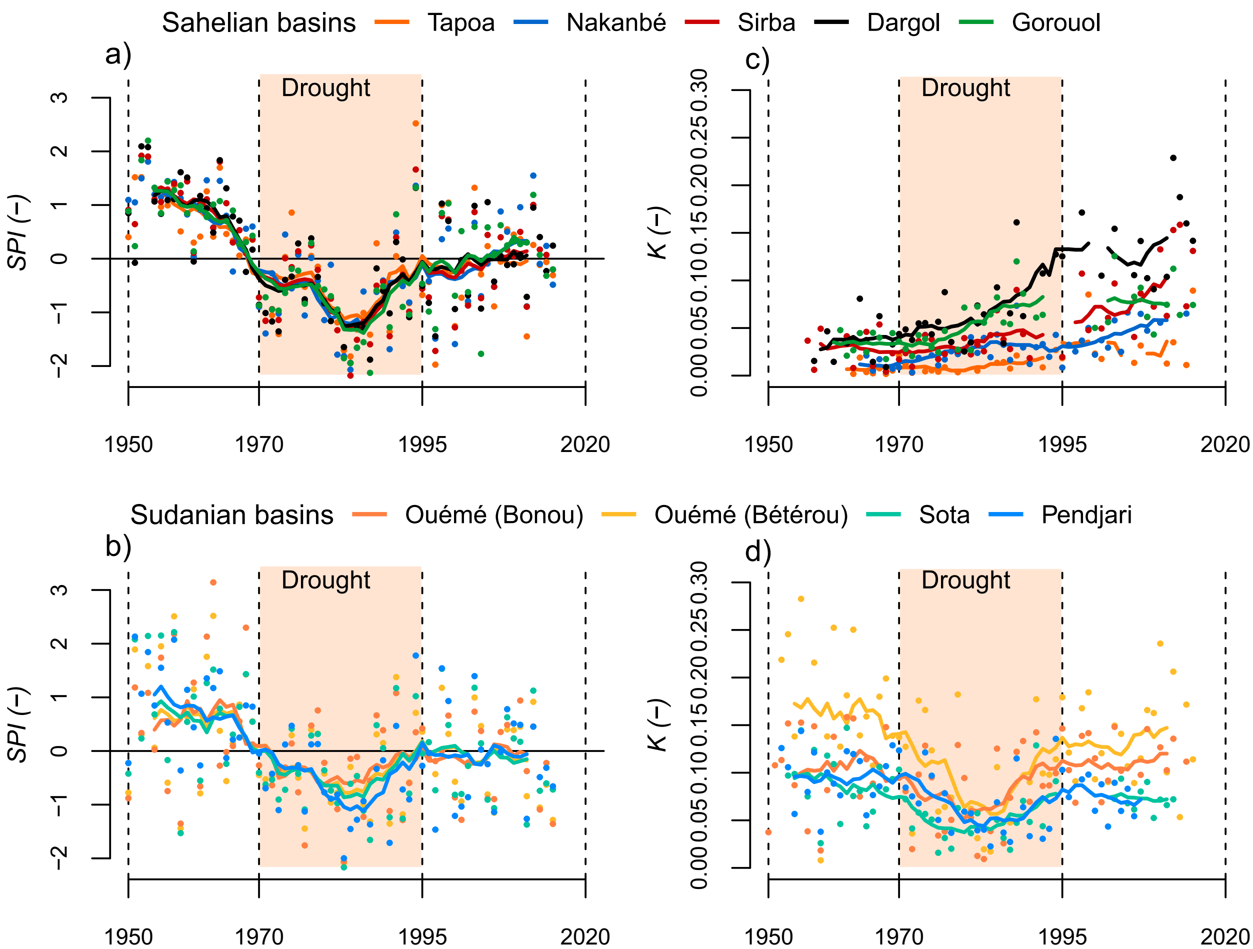

Fig. 2 | Changes in rainfall and runoff in the studied basins between 1950 and 2015. Standard Precipitation Index (*SPI*) over time for the Sahelian (**a**) and Sudanian (**b**) basins, and corresponding annual runoff ratio (*K*) for the Sahelian (**c**) and Sudanian (**d**) basins. Each dot corresponds to one year, and each line represents the centred 9-year moving average, revealing the decadal trend. The lines are broken where missing years prevent the moving average from being computed. The orange area indicates the drought period.

in the four Sahelian basins (Gorouol, Dargol, Sirba and Nakanbé–Fig. 3). This coincides with the beginning of the drought and is consistent with field observations reporting the development and enlargement of bare soil patches[26,50].

All basins have been affected by drought, albeit to varying degrees, as well as by the conversion of natural vegetation into cropland. These localised results are consistent with the trends previously described at the regional scale[13,18,51]. Land cover statistics show no evidence that Sahelian basins have been more affected by land clearing than the Sudanian ones (Table S1). Therefore, land cover alone cannot explain the contrasting behaviour of these two groups of basins.

The analysis of changes in the rainfall–runoff relationship is a common method for identifying hydrological regime shifts[8]. Rather than using runoff volume, we analysed the *P*–*K* relationship between rainfall *P* and the runoff ratio *K* (see 'Methods'), which facilitates comparisons between basins with different orders of magnitude of streamflow.

In the Sahelian basins, *K* remained relatively stable in the 1960s, meaning that streamflow changed proportionally to rainfall (Fig. 4a, 5a, and S1). From the early 1970s onwards, *K* increased despite the drought until around 1985. It continued to increase afterwards, except in the Gorouol basin, where *K* seems to have stabilised as from 1985. The sharp increase in *K* starting around 1990 could be viewed as a specific response to the paroxysm of the drought around 1984. In all of these basins, the post-drought runoff ratio increased two to threefold between 1950 and 2015, moving far beyond the previously observed range of variability. Despite some differences, all the *P*–*K* relationships exhibit a non-monotonous structure, indicating a non-stationary hydrological functioning and strongly suggesting a regime shift (Figs. 4a, 5a, and S1). Based on field and satellite observations[52], the stabilisation in the Gorouol basin is assumed to result from a land fraction where runoff keeps increasing, balanced by a regreening land fraction that partly absorbs additional overland flow.

Conversely, in the Sudanian basins, the relationship between *K* and *P* shows an approximately linear dependence, with *K* decreasing and then increasing as rainfall amounts recovered from 1985 onwards, following the same trajectory back and forth in the *P*–*K* space (Figs. 4b, 5b, and S2). This unchanged *P*–*K* relationship suggests that the hydrological regime has remained stable in these basins throughout the whole period, with a reversible response to rainfall variability.

These contrasting trends are confirmed by the time series of $\frac{K}{P}$, which shows a continuous increase in the Sahelian basins, except in the Gorouol (Supplementary Fig. S3). A trend in $\frac{K}{P}$ indicates that changes in *K* are driven by factors other than the rainfall amount. In the Sudanian basins, the values of $\frac{K}{P}$ before and after the drought are comparable.

Extended datasets for the Sirba basin until 2022 show that the runoff ratio has continued to increase over the last decade and that the decoupling between rainfall and runoff has persisted (Fig. S4). In the

 https://doi.org/10.1038/s41467-026-72648-6

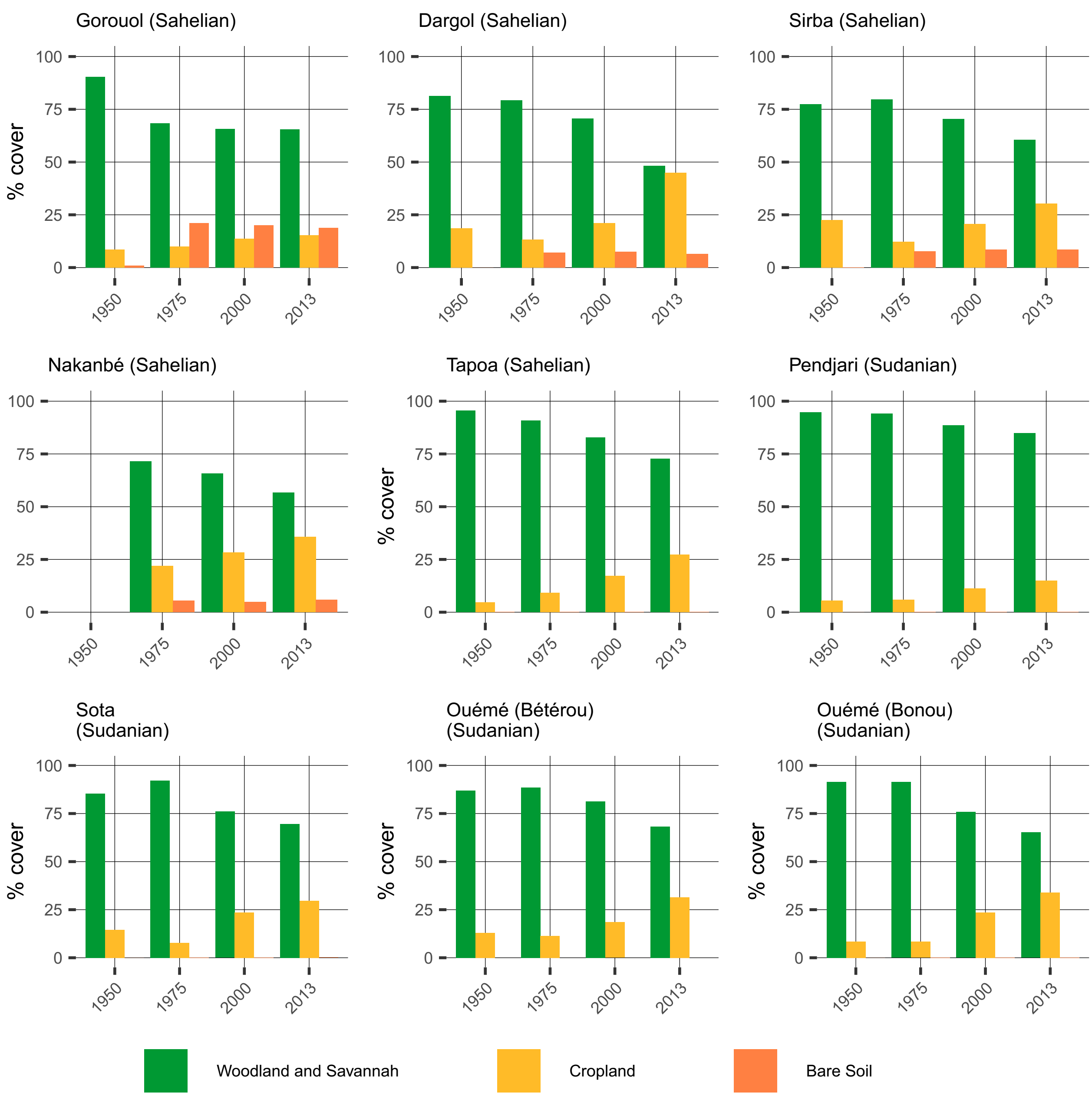

Fig. 3 | Land cover for years 1950, 1975, 2000 and 2013 on each basin. Only the three dominant land cover classes are shown. Others classes represent less than 5% of the basin cover. The subplots are arranged in order of basin location, from north to south (top left to bottom right). 1950 data for the Nakanbé basin are not available.

Ouémé (Bétérou) basin, the *P*–*K* relationship appears to have evolved over the past 15 years, with a higher *K* value observed for comparable rainfall levels than prior to the mid-2000s. However, *K* remained within the same variability range observed since 1950. This behaviour emerged about 10 years after the end of the drought in the mid-1990s. Given this time lag, it is unlikely that this change is a consequence of the drought. We hypothesise that it is instead the result of an increasing proportion of cropland in the basin, combined with more intense rainfall. Further analysis is required to investigate this recent change.

Regime shift detection

In a system with multiple alternative states, regime shifts lead to multimodality in the distribution of the variables that describe the regime[53]. We define a basin as having shifted to a high runoff state if, after a perturbation, the range of values of *K* is significantly higher than in the previous state, and this new state persists beyond the end of the perturbation that caused the shift. A shifted basin is expected to remain in its new state indefinitely unless a new perturbation or other factors cause it to evolve differently. The observations show that there are two regimes in the Sahelian basins, corresponding to low and high runoff, and that the largest changes in these basins occurred between the pre- and post-drought periods. Therefore, we simply tested whether the statistical distribution of the runoff ratio *K* was significantly different between periods, using the Wilcoxon two-sample test (see 'Methods'). We applied the same method to other variables to check for regime shifts in the forcing.

For all basins, the annual rainfall during the drought was significantly lower than in the preceding period (Fig. 6a and Table S3). Despite the relative recovery in the last period, the annual amounts remained significantly lower than before the drought (Table S2). However, the recovery was more significant in the Sahel than in the

https://doi.org/10.1038/s41467-026-72648-6

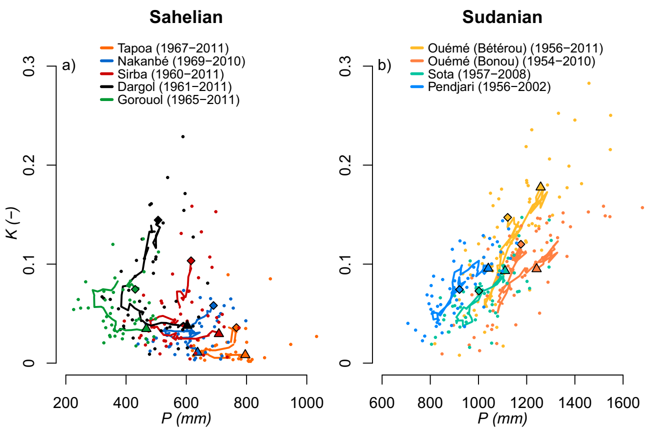

Fig. 4 | Annual rainfall–runoff (*P*–*K*) relationships. Dots represent *P* and *K* values, and lines the 9-year centred moving average on both *P* and *K*, revealing the decadal trend, for the Sahelian (**a**) and Sudanian (**b**) basins. The lines may be broken for some basins due to missing years. The triangles and diamonds correspond to the start and stop of the time course given in brackets. This time course starts 4 years later and stops 4 years earlier than the full dataset due to averaging.

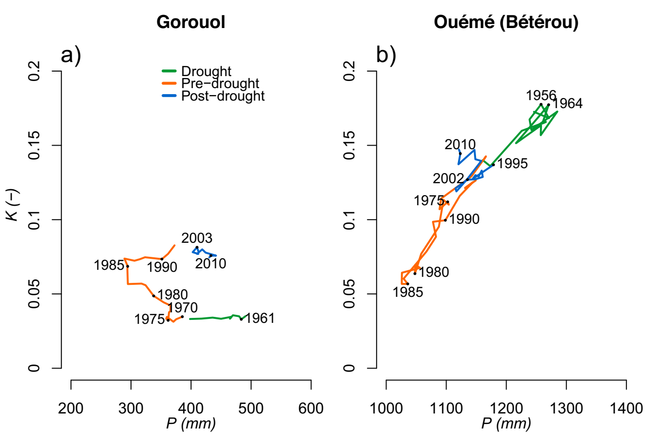

Fig. 5 | Annual rainfall–runoffrelationships for two selected basins. Same as Fig. 4 for the Gorouol (**a**) and Ouémé (Bétérou) (**b**) basins. Only the 9-year moving average line is shown, with selected date markers along the time course (dates are at the centre of the moving window). The green, orange and red colours correspond to the pre-drought, drought and post-drought periods, respectively. The turning point in 1985 roughly coincides with the drought peak.

southern basins (Table S4). These patterns are confirmed by the distribution of *SPI* between periods (Fig. 6b). On all the basins, *SPI* reached values as low as −2, indicating severe drought conditions[54], with several consecutive dry years with $SPI < -1$ between 1982 and 1987 (Table S5).

Regarding runoff ratios, the distributions of *K* between the pre- and post-drought periods are statistically different for all the Sahelian basins (Fig. 6c and Table S2). The change is also significant between the drought and post-drought periods (Table S4). This confirms that a hydrological regime shift towards a higher runoff for a similar annual rainfall has occurred in the Sahelian basins.

In the Sudanian basins, the distributions of *P* and *K* also differ significantly between the pre-drought and drought periods (Fig. 6a, c and Table S3), but not any more between the pre- and post-drought periods (Fig. 6a, c and Table S2). This indicates that the Sudanian basins have recovered similar operating conditions to those before the drought, with no evidence of a regime shift.

As reported at the regional scale, rainfall intensity has increased since the mid-1990s[18]. This trend has also been observed in the study basins, as shown by the changes in the hydro-climatic index *HCI* (see 'Methods'). The *HCI* is higher when the same amount of annual precipitation is brought by fewer but more intense events. This index was significantly higher after the drought than before in all the basins (Fig. 6d and Table S2). Intensification mostly occurred between the pre-drought and drought periods (Table S3 and S4), with the largest changes in *HCI* occurring in the northernmost Sahelian basins (Fig. 6d). Higher rainfall intensity generates more runoff, and intensification of rainfall has probably contributed to the runoff trend in the Sahelian basins, and also in the Sudanian basins, although intensification was less pronounced there.

When a regime shift occurs, it is often associated with a triggering event. Indeed, the rainfall deficit has led to an increase in aridity, as described e.g. by the aridity index AI^* (see 'Methods'). Drought has caused an aridity shock in all basins, which has been more severe in the Sahel than in the southern part of the region (Fig. 6e). Berdugo et al.[55] have identified three aridity thresholds that, when crossed, can trigger regime shifts in dryland ecosystems: 'systemic breakdown' ($AI^* = 0.80$), 'soil disruption' ($AI^* = 0.69$), and 'vegetation decline' ($AI^* = 0.54$). In the two northernmost basins, Dargol and Gorouol, the breakdown threshold ($AI^* = 0.80$) was exceeded for 5 and 12 consecutive years, respectively (Table S6). In these two basins, as well as in the Sirba, the intermediate threshold ($AI^* = 0.69$) was exceeded in more than 70% of the drought period, and during 11 to 25 consecutive years. The lowest threshold was exceeded for 8 consecutive years in the Pendjari basin, but none of the three thresholds was exceeded in the southernmost Sota and Ouémé basins.

The aridity gradient is consistent with the strength of the hydrological shift (Fig. 6). The most severe impacts were observed in the four northernmost basins (Dargol, Gorouol, Sirba and Nakanbé), which are also those where a significant fraction of bare soil has developed (Fig. 3). Although these aridity thresholds were defined from a completely different ecological perspective, they correspond well with the contrasting changes amongst the basins. The value $AI^* \approx 0.7$ seems to be a critical limit beyond which aridity induces systemic eco-hydrological changes. These results suggest that the prolonged aridity associated with the rainfall deficit was most likely the main trigger of the regime shift.

While it is generally difficult to prove the existence of alternative regimes from field data alone[53], the shift is established in these basins, given the 2–3 fold increase in the runoff per unit rainfall, the persistence of the new regime for over 20 years after the end of the drought, and the comparison with the Sudanian basins, which did not shift. Building on these results, we propose a conceptual model to support the RS hypothesis and the interpretation of the observed hydrological changes as a transition between states. The model is based on two feedback loops (Fig. 7). The first is a local-scale balancing loop (*B*) in which the infiltration of runoff over short distances (typically 10–100 m) provides neighbouring vegetation with resources, such as water, seeds, nutrients, soil particles and organic matter. Thereby, it facilitates vegetation maintenance and prevents erosion and the expansion of runoff-prone bare soil areas[56–58]. This feedback loop stabilises the low-runoff state at the local scale. Patterned vegetation, which is common in drylands worldwide[59], is a good example. In the central Sahel, streamflow primarily originates from Hortonian surface runoff, which occurs when rainfall intensity exceeds the soil hydraulic conductivity[60]. Due to this priority partitioning of rainfall, surface runoff is the main contributor to streamflow, with minimal contributions from baseflow[23,61,62]. Consequently, the *B* loop also stabilises the low-runoff state at the basin scale.

The second is a reinforcing loop (*R*) where surface runoff propagates over longer distances, either because of the extent of runoff-prone areas or their hydrological connectivity, defined as the length of connected pathways for runoff, wind and water erosion[63]. The resulting loss of local resources prevents vegetation survival, thus favouring runoff[56–58,63]. Soil crusting tends to develop on bare surfaces exposed

https://doi.org/10.1038/s41467-026-72648-6

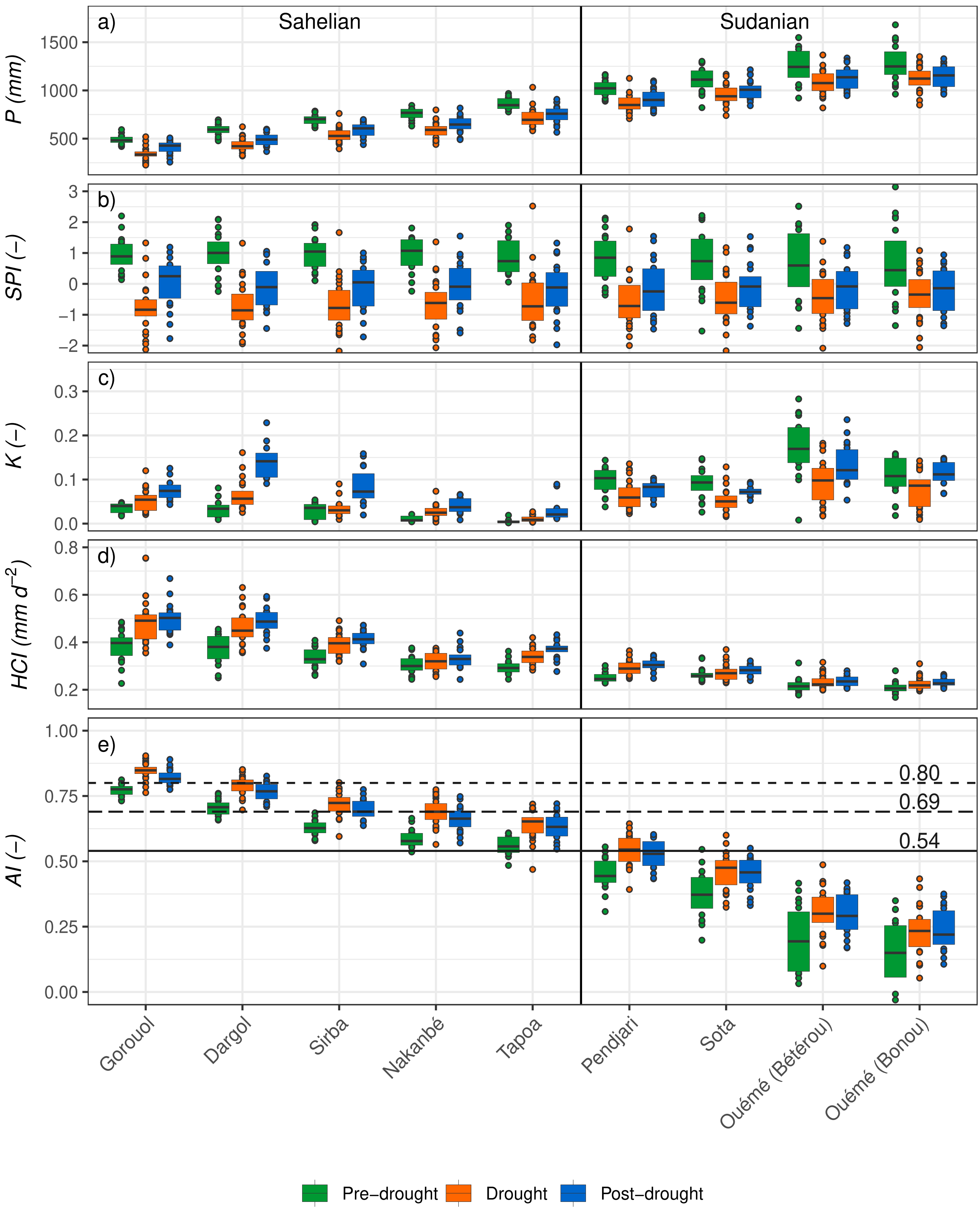

Fig. 6 | Comparison of hydro-climatological indices for the three periods. Boxplot (median, 25th and 75th percentiles) and data points for annual rainfall *P* (**a**), Standard Precipitation Index *SPI* (**b**), runoff ratio *K* (**c**), hydro-climatic intensity *HCI* (**d**) and aridity index AI^* (**e**) for the three periods in each basin. Basins are ordered by decreasing latitude on the horizontal axis (northernmost left, southernmost right). The horizontal lines in (**e**) show the critical thresholds for ecosystem resilience to drought proposed by Berdugo et al.[55].

to the high intensities of tropical rainstorms[64,65], reducing soil hydraulic conductivity and thus favouring local surface runoff and erosion[66,67]. Local erosion in turn leads to the progressive development of rills and gullies, connecting runoff-prone areas, and further increasing hydrological connectivity at larger scales. Once established, self-sustaining hydrological connectivity and gully networks are unlikely to disappear naturally, without major environmental (geomorphological, climatic) changes or human intervention. This feedback

https://doi.org/10.1038/s41467-026-72648-6

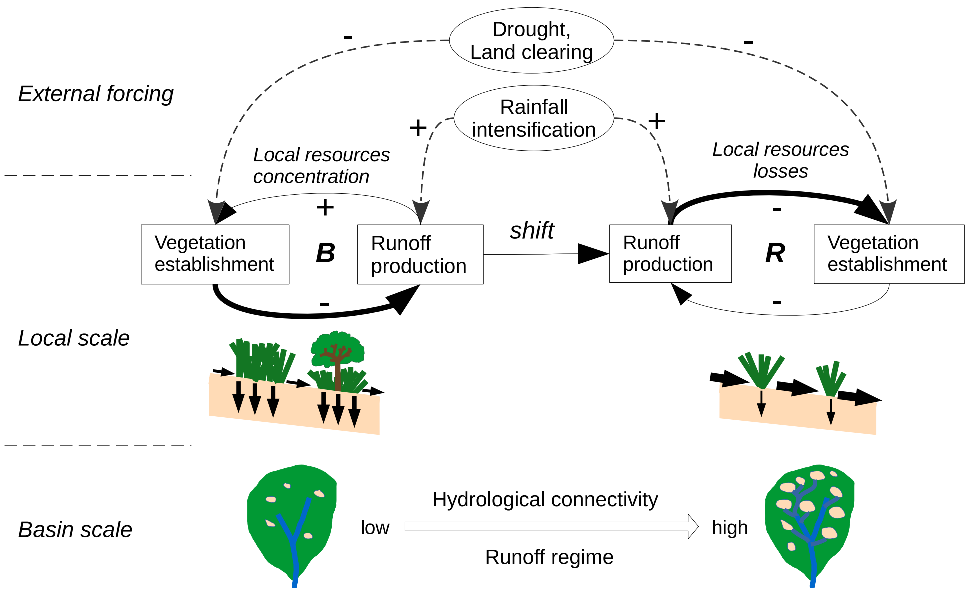

Fig. 7 | Conceptual model supporting the RS hypothesis. The arrows show the relationships between elementary processes: dominant processes (bold arrows) and effects of changes in external forcing (dashed arrows). The '+' and '−' signs indicate the direction of the change along the arrows: '+' means that both variables co-evolve, and '−' means they evolve in opposite ways. *B*: Balancing (negative) feedback loop, where vegetation limits runoff and thus favours local infiltration, which in turn favours vegetation establishment by concentrating resources locally (see text). *R*: Reinforcing (positive) feedback loop, where increased runoff exports resources on a larger scale, which is detrimental to the survival or expansion of vegetation. This, in turn, increases runoff and favours the development of hydrological connectivity. Feedback loops *B* and *R* stabilise the low and high runoff regime, respectively. When perturbations in the forcing cause vegetation loss or local runoff increase beyond thresholds, the equilibrium in the *B* loop is disrupted, and the *R* loop becomes dominant, inducing a shift from the low to the high runoff regime. The diagrams in the middle panel illustrate the change in the partition of water between runoff and infiltration associated with each loop at the local scale. The lower panel shows how the development of the hydrological network (blue) and the connectivity of runoff-prone areas (pale) affect the basin runoff regime.

loop therefore stabilises the high runoff state at both local and basin scales. If an external factor reduces vegetation, the limiting effect of vegetation on surface runoff decreases, and beyond critical conditions, the balancing loop (*B*) is disrupted (Fig. 7). This eventually results in the reverse process (*R* loop) becoming dominant, whereby surface runoff prevents vegetation development, resulting in a shift to the high runoff regime.

This conceptual model enables us to propose a narrative that describes the hydrological dynamics of the central Sahel over the past seven decades. In the 1950s, all the basins were in the low-runoff state, with annual runoff ratios lower than 5% (Figs. 2c and 4a). Local stabilising processes (*B* loop) were dominant, with most of the rainfall infiltrating within the hillslopes. In the second phase, starting in the 1970s, the drought and the associated aridity shock caused vegetation to die off[26,50,68]. The conditions that destabilise this loop prevailed, resulting in a progressive shift towards the alternative state. This phenomenon was exacerbated by anthropogenic land clearing in the areas suitable for rainfed agriculture. During the drought and the following wetter phase, greater annual rainfall amounts, higher intensities and sustained agricultural activity, combined with the persistence of bare soil areas, contributed to maintaining the high-runoff regime through the *R* loop. This conceptual model may also be relevant in other areas, since the feedback loops in Fig. 7 have been identified in various drylands[56–58,63].

Discussion

A number of field evidence supports the RS hypothesis and the conceptual feedback model. An increase in local runoff in the central Sahel was first reported in the mid-1980s[13]. The expansion of areas of bare soil seen in land cover maps (Fig. 3) has also been observed in the field[26]. Gullies development and increased hydrological connectivity have been reported in various locations[24,25,69]. In southwestern Niger Leblanc et al.[19] reported a 2.5-fold increase in drainage network density between 1950 and 1992. Similarly, in northern Mali, Trichon et al.[68] reported a 4.3-fold increase in the drainage network density of a tiger bush system between 1955 and 2015.

The regreening of the Sahel in the post-drought period may appear to conflict with the runoff trend, since vegetation recovery should hinder runoff generation. However, field observations show that the landscape has become fragmented[26,50]. Runoff-prone areas have appeared in the most vulnerable locations (e.g. rocky soils, hard pans and shallow sandy soils), scattered throughout areas with more favourable conditions, such as deep sandy soils, where regreening has taken place. These scattered bare patches play a key role in supplying water to the drainage network, particularly when interconnected by gullies. Large bare soil areas are easily identified in satellite-based land cover maps (Fig. 3), but the numerous bare patches of limited size cannot be detected by the vegetation indices such as NDVI used to evidence regreening[26,28]. Reasoning with feedback loops, this fragmented landscape corresponds to the spatial coexistence of expanding runoff-prone areas, driven by the *R* loop and connected to the drainage network, and areas where conditions are favourable to infiltration and vegetation establishment, driven by the *B* loop (Fig. 7). Thus, this patchy behaviour resolves the apparent contradiction between regreening and increased runoff. The local regime shifts can be triggered quickly (e.g. after a few heavy rainstorms), but their impact on the hydrological cycle at larger scales emerges gradually, through the progressive expansion of bare areas and hydrological connectivity. Our results (Supplementary Fig. S1) and those of Wendling et al.[40] suggest that a shift can develop over a period of one to two decades.

The stationarity of the rainfall-runoff relationship in the Sudanian basins—i.e. the absence of shift—is related to a series of differences with the Sahelian context. Streamflow in these basins primarily originates from the discharge of near-surface (approximately 2 m deep) perched seasonal water tables that are recharged annually.

Contribution from Hortonian runoff and permanent deep groundwater is minimal[70,71]. On an annual timescale, this results in streamflow responding quickly and directly to rainfall[61]. Soils in the Sudanian area are less susceptible to crusting and degradation than those in the Sahel due to their clay mineralogy, higher organic matter content and stronger biological activity[65]. In Sudanian savannas, tree cover is denser than in the Sahel, and grass species are mostly perennial. In this energy-limited region, soil water is not a limiting factor for vegetation[72]. Lastly, despite the rainfall deficit, aridity levels remained moderate in this region (Fig. 6e and Table S6). All these factors enabled the Sudanian basins to withstand this prolonged drought.

Although the RS hypothesis seems sufficient to explain the shift, alternative hypotheses could be considered. Increased runoff could be due to a change in the balance between evapotranspiration (*ET*), underground storage and baseflow. *ET* has been increasing across the entire Sahel since the 1980s[73], and soil moisture resets to its minimum each year during the dry season[74]. Thus, these two factors cannot cause an increase in runoff. Groundwater recharge is seasonal and sensitive to rainfall extremes[75], but there is no indication of a long-term rise in the water table in Sahelian basins over crystalline bedrock[76,77]. Moreover, the water table typically lies below the stream network, and is recharged by the intermittent streams rather than drained by them[76]. Lastly, given the low permeability of these crystalline aquifers[46,77,78], the contribution of groundwater to streamflow is very limited, if any. Therefore, the regime shift could not be driven by substantial interactions between *ET* and underground processes. Alternatively, the high-runoff state in the Sahelian basins could be merely a transient behaviour driven by the inertia of some basin compartments. However, it is difficult to imagine an inertial process, independent of underground storage, that would lead to a persistent change more than 20 years after the end of the drought. The return flow associated with groundwater pumping for irrigation is also not a factor here, as there are no large-scale irrigation systems in this area[48,49].

A more plausible alternative is that the high-runoff state is simply a response to higher rainfall intensities falling on runoff-prone land fractions, either inherited from the drought or from human-induced land cover change. Hortonian runoff increases non-linearly with rainfall intensity, and extreme rainfall has increased by about 5% per decade since the mid-1980s[79]. Agriculture and the loss of natural vegetation due to land clearing are recognised as factors contributing to land degradation[80]. In the Sahel, weeding in crop fields alters the stability of soil aggregates and exposes the soil surface to raindrops, favouring soil crusting[64]. Weeding improves infiltration only temporarily as crusting is restored after a few rains[81]. Wind erosion may also play a role in maintaining or enlarging bare soil surfaces. Indeed, the expansion of cropland in the Sahel has been identified as the cause of increased runoff[13,19,20,23,62]. High runoff conditions also persist in the northernmost grass savannahs (e.g. the Gorouol basin), where croplands are scarce and extensive cattle grazing, practised in this area for centuries, mostly preserves the ecosystem and is unlikely to cause soil degradation[24–26,50]. In this region, human activity has little impact on land cover change, and the observed changes are mostly due to climatic factors. When considered as external factors, rainfall intensification and/or land cover changes could drive the regime shift, particularly in the post-drought period. However, as illustrated in Fig. 7, any factor that directly decreases vegetation cover or increases runoff could trigger or maintain a shift to the high-runoff state. Therefore, changes in land cover, combined with higher rainfall intensity, can also play as an internal factor involved in the feedback mechanisms. For these reasons, these two factors are not a real alternative to the RS hypothesis but, instead, part of it. In fact, they are confounding factors, and assessing their detailed contribution to the shift requires a modelling approach.

Several studies in the same region have successfully reproduced the runoff trend in the Central Sahel using standard hydrological models (i.e. with no feedback) and observed climate and land cover time series as forcing factors[21,25]. Some of these studies suggest that the main drivers of increased runoff were land cover change during the drought, and rainfall intensification afterwards[22,62]. However, these approaches cannot be used to test the RS hypothesis since they only simulate the response to rainfall for prescribed surface conditions and do not take into account the dynamic interactions between rainfall, soil and vegetation. Conventional hydrological models implicitly assume a single regime and do not represent feedback mechanisms[11]. Using a system dynamics modelling based on the principles of the conceptual model proposed in Fig. 7, Le Roux et al.[82] reproduced the regime shifts in these Sahelian basins with annual rainfall as the sole forcing. They clearly identified two runoff regimes and a shift between them, and showed that the drought was sufficient to trigger this shift. These results confirm the relevance of this type of modelling approach for regime shift studies. Future developments accounting for diverse rainfall intensity regimes, drought configurations (e.g. duration and rainfall deficit) and land cover scenarios will help to determine the conditions that trigger or prevent a shift in both the Sahelian and Sudanian contexts. This will also contribute to anticipating possible future hydrological trajectories.

Our two-state model appears well-suited to explaining cases where some basins recover from drought, while others do not. Such a contrasting behaviour has also been reported in Australia by Peterson et al.[11], where basins shifted towards a low-runoff regime as a consequence of the Australian Millennium Drought, while others recovered. Despite these similarities, there are significant differences between the two cases. In the Australian basins, this shift has been attributed to a change in rainwater allocation through increased evapotranspiration (ET) per unit of precipitation, leaving less water available for streamflow[11,83]. This resulted in a shift in the opposite direction to that observed in the Sahel. The recovery of the Australian basins has not been clearly elucidated, although replenishment of subsurface storage is likely to have been involved. Conversely, our study shows that the shift in these Sahelian basins is associated with persistent changes in the land surface properties in a context where streamflow is dominated by overland flow, with virtually no groundwater contribution, which explains the direction of the shift. Incidentally, it is inappropriate to consider that the Sudanian basins have recovered from drought, since no temporary deviation from the historical relationship between precipitation and runoff has been observed. Instead, runoff has rapidly and proportionally adjusted to changes in rainfall, preserving the dependence of K on P. However, it is unclear how these basins would respond if conditions for a shift were to occur, depending on whether land surface processes, underground processes, or a combination of both become dominant. Although the observations document a shift from the low- to the high-runoff state in the Sahelian basins, a reverse shift is theoretically possible. A model assessment of the conditions for triggering such a back shift would be useful, for example, when designing unconventional, nature-based land restoration solutions based on feedback mechanisms[84].

Methods

Basin selection

The basins selected in this study span the West African ecoclimatic gradient, from 300 mm of mean annual precipitation in the north to 1200 mm in the south (Table 1). They were selected because they have the longest, multi-decadal time series of annual rainfall and runoff. The basin boundaries were extracted from the ADHI database[85]. A large part of the west of the Gorouol basin is purely endorheic and does not contribute to discharge at the basin outlet. Its boundary was corrected based on expert elicitation to only consider the part that actually contributes to the basin outflow. The Ouémé (Bétérou) basin is the upper part of the Ouémé (Bonou) basin, accounting for 20% of its area. However, its contribution to the discharge at Bonou is very small (<10%

on average) and its rainfall pattern (one single rainy season) is different from that of the Bonou basin (two rainy seasons). Therefore, these basins were considered independent with regard to the changes analysed in this study. The Gorouol, Dargol, Sirba, Tapoa and Sota basins are part of the great Niger River basin, whereas the Nakanbé and Pendjari basins belong to the Volta River system. The mouth of the Ouémé River is located southeast of the Bonou outlet in the Atlantic Ocean.

Delimitation of the three periods

The year 1950 coincides with the beginning of most of the rainfall and runoff datasets and with the oldest land cover maps. Hence, it was set as the beginning of the study period. Similarly, the year 2015 (end of our study period) is the best compromise for the availability of both rainfall and runoff data we can access. There is a broad consensus in the literature that the West African drought began around the year 1970, with variations of only 1 to 2 years depending on the study[15,16,86]. The end of the drought is less clear because the rebound in annual rainfall amounts has been gradual and also because of the regional variability in this rebound[18]. It corresponds to an intensification of rainfall that started in the early 1990s, with fewer but larger and more intense events leading to a net increase in annual rainfall relative to the drought period, but still below pre-drought level[51,87,88]. We adopted 1994 as the end of the drought, which is a compromise between the starting year of the new rainfall regime used in different studies[18,86,89,90]. Therefore, we defined the three periods as follows: the pre-drought period from 1950 to 1969 (20 years), the drought period from 1970 to 1994 (25 years), and the post-drought period from 1995 to 2015 (21 years).

Land cover

Two data sources were merged to assess land cover changes over the study period. First, we used the USGS West Africa Land Use Land Cover Time Series[17]. This 2-km resolution reference dataset was produced by photo-interpretation of Landsat images. It describes land cover in 1975, 2000, and 2013 across West Africa, using a classification system with 26 categories. This USGS product was chosen due to its homogeneity over a period of around 40 years. It covers the drought and post-drought periods. Second, to complement this series and align it with the hydrological dataset, we produced land cover maps of the study basins prior to the drought using an original method. We digitised the 1950s editions of the 1:200,000 topographic maps published by IGN (National Geographic Institute, France) covering the whole study area (36 maps). Each map covers an area of 1° × 1°. The background of these maps was carefully documented by IGN staff using stereoscopic, panchromatic aerial photographs at 2–3 m horizontal resolution taken between 1949 and 1952 (depending on the maps), covering the entire studied region. The resulting digitised raster files were mosaicked and geo-referenced. The original legends of these 36 maps were homogenised by expert elicitation to provide a final series of 13 land cover categories. These maps revealed a relatively accurate documentation of the main categories, including settlements and a clear distinction between natural vegetation and cropland.

The IGN and USGS maps were projected to a common 15-m resolution. As the study focuses on land conversion for cropping and land degradation, the initial land cover categories from the two sources were merged into three general categories: 'woodland and savannah', 'cropland' and 'bare soil'. For each basin, the cover fraction of each of the three categories was extracted using Python GIS libraries.

In some basins (Sirba, Sota and Ouémé to a lesser extent), woodland and savannah cover increased slightly between 1950 and 1973, while the proportion of cropland decreased (Fig. 3). It is difficult to say whether this reflects a real process or uncertainties due to the different nature and data processing of the IGN and USGS data sources. Agroforestry is a traditional farming system throughout the region, where trees are maintained in the fields. Agroforestry plots and open savannahs can be difficult to separate in remote sensing datasets. This leads to uncertainties in the coverage estimates for the savannah and field classes in the Landsat-derived land cover maps. However, these uncertainties do not alter the long-term trend of increasing area under cultivation.

The W National Park, established in 1954, covers about 25% of the Tapoa basin. Similarly, the Pendjari National Park, established in 1961, covers about 37% of the Pendjari basin. Therefore, these two basins are not affected by agricultural expansion within the protected areas, resulting in a low proportion of cropland (Table S1).

Rainfall and runoff data

Precipitation. Precipitation datasets were extracted from the BADOPLU database, covering the period 1950–2015. This database and the methods for processing rainfall data are detailed in the supplementary material of Panthou et al.[18]. In summary, for each basin, annual precipitation P was estimated from rain gauge observations in two steps. Daily precipitation from rain gauge stations included and bordering each basin was spatially interpolated using a kriging technique, which accounts for anisotropy in the precipitation field. The basin daily precipitation was computed as the areal mean of the interpolated field over the basin. The annual precipitation is the sum of the daily rainfall over the hydrological year, starting on 1 March. The three indexes below have been calculated using the same definition of the hydrological year.

Precipitation index. The dimensionless Standardised Precipitation Index *SPI*[54] is widely used to characterise droughts. It allows comparison of rainfall series between different basins. In the general case, a probability distribution (e.g. gamma) is first fitted to the rainfall data, and an anamorphosis is applied using the inverse normal transformation in order to associate with each rainfall value the equivalent percentile in a normal distribution. However, we verified that the mean annual rainfall on each basin is normally distributed (Table S7). Therefore, there is no need to transform the original data, and the *SPI* is defined for each basin as the difference between the annual rainfall of the current year P (mm) and its inter-annual mean $\overline{P}$ (mm), normalised by its standard deviation $\sigma(P)$ (mm), both computed over the whole 1950–2015 period. It writes:

$$\mathrm{SPI} = \frac{P - \bar{P}}{\sigma(P)} \tag{1}$$

Hydro-climatic intensity. The hydroclimatic intensity HCI (mm d^{-2}) is defined as the ratio between the mean rainfall during wet days $\overline{P_{\mathrm{wet}}}$ (mm d^{-1}) and the number of wet days N_{wet} (time, in days) during the year[18]:

$$HCI = \frac{\overline{P_{\mathrm{wet}}}}{N_{\mathrm{wet}}} \tag{2}$$

A day is considered wet if the amount of precipitation exceeds 0.5 mm. $\overline{P_{\mathrm{wet}}}$ is the ratio between the total amount of precipitation on wet days and the number of wet days N_{wet}. A low *HCI* indicates that the year's rainfall is made up of many low-intensity events, while a high *HCI* corresponds to fewer but more intense rainfall events.

Aridity index. The aridity index $AI^*(-)$ used in this study is defined as the complement to the ratio of annual rainfall P (mm) to potential evapotranspiration PET (mm):

$$AI^* = 1 - \frac{P}{PET} \tag{3}$$

This definition is similar to the aridity index used by Berdugo et al.[55]. The star superscript avoids confusion with alternative definitions of this index, such as $AI = \frac{P}{PET}$. AI' varies between 0 and 1, and increases with aridity, either due to low rainfall or high potential evaporation. For P we used the annual precipitation over each basin. For PET, we used hourly PET calculated with the algorithm of Singer et al.[91], using meteorological fields retrieved from the ERA5-Land reanalysis[92]. This covers the period from 1950 to the present day, with a grid resolution of 0.1°. The hourly PET values were summed over the hydrological year and then averaged spatially over the boundary of each basin using the *raster* package, in the *R* environment (version 4.4)[93].

Runoff. Except in the large Niger and Volta rivers, the rivers in the study area are intermittent, flowing only during the monsoon rainy season, with no or very low flows during the dry season (Table 1). The annual discharge Q ($m^3\,yr^{-1}$) was calculated from the mean daily discharge Q_{daily} over a hydrological year, starting on 1 March. The daily discharge time series were extracted from SIEREM[94], ADHI[85] and the AMMA-CATCH databases[43] for all basins except Nakanbé. The datasets retrieved from those databases were merged to obtain the longest time series. For the Nakanbé basin, we used naturalised data with discharges corrected for the effect of the dams that were built as from the mid-1980s, obtained from Gbohoui et al.[62].

The number of streamflow stations in West Africa has decreased over the past seven decades, and the quality of the datasets has deteriorated[95]. This decline has been particularly severe from the early 1980s onwards[85]. These constraints strongly limited the selection of long enough series of records of annual rainfall and runoff covering the entire study period. To avoid rejecting too many series, limited curation and gap-filling operations were performed. Data curation consisted of reconstructing a few missing Q_{daily} values in the dry season (set to 0 if no flow observations were available before and after) and in the recession limb of each hydrograph at the end of the wet season, which were approximated by a decreasing exponential function fitted to the recession limb for years without gaps at the same station. After this gap-filling stage, years with periods of missing consecutive daily values longer than 13 days were excluded from the database, and data gaps shorter than 13 days were reconstructed by linear interpolation. A sensitivity study on complete years showed that this interpolation had a limited effect, with a relative bias of less than 10% on the calculated mean annual discharge. The availability of streamflow data for each basin is given in Table 1.

The annual runoff ratio K (−) is defined as the ratio between the annual water yield $\frac{Q}{S}$ ($m\,yr^{-1}$) and the annual rainfall P ($m\,yr^{-1}$):

$$K = \frac{1}{P} \cdot \frac{Q}{S} \tag{4}$$

where S (m^2) is the basin area. This dimensionless quantity takes into account the first-order linear dependence of runoff on rainfall, making it possible to compare basins under different climatic conditions.

For two basins, we obtained privileged access to more recent streamflow records from the Niger Basin Authority (ABN) and the AMMA-CATCH observatory. These records extend to the end of the 2022 hydrological year for the Sahelian Sirba basin, and to the end of the 2023 hydrological year for the Sudanian Ouémé (Bétérou) basin. Since there are no BADPOLU datasets for this period, we derived the corresponding annual rainfall from the CRU database[96] (see Fig. S5).

Statistical tests

In order to compare the distribution of the different metrics (rainfall, *SPI*, runoff ratio, hydroclimatic and aridity indexes) between two periods, we used the unpaired Wilcoxon rank sum test, also known as the Mann–Whitney test[97]. This non-parametric test, based on ranks, is used to compare two samples of independent values drawn from an unknown statistical distribution. The null hypothesis H0 is that the two samples are drawn from the same distribution. We used a significance level of 0.05; thus, we reject H0 for p-values lower than this level. For the comparisons between periods, we used the two-sample version of the test, assessing only whether the two distributions were different, rather than whether the values of one distribution were higher or lower than the values of the other. For the AI', we used the one-sample version of the same test to assess whether the distribution of AI' in the drought period was significantly higher than each of the three thresholds (0.8, 0.69 and 0.54). The tests were performed with the *stats* package under the *R* statistical computing and graphics environment (version 4.4).[93]

Data availability

The rainfall datasets (1950–2015) were obtained from Panthou et al.[18]. The CRU TS4 rainfall datasets (2016–2023) are available at https://catalogue.ceda.ac.uk/uuid/9cf07e92afaa405da4f40b6733f362d3. The ERA5-Land *PET* datasets are available at https://cds.climate.copernicus.eu/. Streamflow data for the Ouémé (Bétérou) basin is available at https://www.amma-catch.org under https://doi.org/10.17178/AMMA-CATCH.CL.Run_O. Streamflow data for the Nakanbé basin was obtained courtesy of the Directorate General of Water Resources, Ministry of Environment, Water and Sanitation of Burkina Faso, from Gbohoui et al.[62]. Streamflow data from 2016 to 2022 on the Sirba basin was obtained from the Niger River Authority. All other streamflow datasets were obtained from the SIEREM and the databases. The basin boundaries in Fig. 1 are available from https://dataverse.ird.fr/dataverse/BvAfriqueCentraleHSM. The land cover datasets for 1973, 2000 and 2013 are available at https://www.usgs.gov/data/west-africa-land-use-land-cover-time-series. The 1950 land cover was digitised for this study from 1:200,000 scale ancient topographic maps published in the 1950s by IGN (National Geographical Institute, France). Due to third-party regulations regarding data dissemination, the rainfall and runoff datasets produced during this study cannot be made public. However, they are available from the corresponding author upon request.

References

1. Scheffer, M. et al. Catastrophic shifts in ecosystems. *Nature* **413**, 591–596 (2001).
2. May, R. M. Thresholds and breakpoints in ecosystems with a multiplicity of stable states. *Nature* **269**, 471–477 (1977).
3. Sguotti, C. & Cormon, X., Regime shifts - A global challenge for the sustainable use of our marine resources. In (eds Jungblut, S., Liebich, V. & Bode, M.) *YOUMARES 8 - Oceans Across Boundaries: Learning from Each Other*, 155–166 (Springer International Publishing, 2018).
4. Mata, S., Braga, J. M. A., Flores, B. M. & Sansevero, J. B. B. Use of the alternative stable states concept in tropical terrestrial ecosystem research-A systematic literature review. *Biotropica* **57**, e70025 (2025).
5. Lenton, T. M. et al. Tipping elements in the Earth's climate system. *Proc. Natl. Acad. Sci. USA* **105**, 1786–1793 (2008).
6. Armstrong McKay, D. I. et al. Exceeding 1.5°C global warming could trigger multiple climate tipping points. *Science* **377**, eabn7950 (2022).
7. Milkoreit, M. Social tipping points everywhere?-Patterns and risks of overuse. *WIREs Clim. Change* **14**, e813 (2023).
8. Tian, W., Liu, X., Liu, C. & Bai, P. Investigation and simulations of changes in the relationship of precipitation-runoff in drought years. *J. Hydrol.* **565**, 95–105 (2018).
9. Avanzi, F. et al. Climate elasticity of evapotranspiration shifts the water balance of Mediterranean climates during multi-year droughts. *Hydrol. Earth Syst. Sci.* **24**, 4317–4337 (2020).
10. Alvarez-Garreton, C. et al. Progressive water deficits during multi-year droughts in basins with long hydrological memory in Chile. *Hydrol. Earth Syst. Sci.* **25**, 429–446 (2021).

11. Peterson, T. J., Saft, M., Peel, M. C. & John, A. Watersheds may not recover from drought. *Science* **372**, 745–749 (2021).
12. Zipper, S. et al. Alternative stable states and hydrological regime shifts in a large intermittent river. *Environ. Res. Lett.* **17**, 074005 (2022).
13. Descroix, L. et al. Spatio-temporal variability of hydrological regimes around the boundaries between Sahelian and Sudanian areas of West Africa: a synthesis. *J. Hydrol.* **375**, 90–102 (2009).
14. Descroix, L. et al. Evolution of surface hydrology in the Sahelo-Sudanian strip: an updated review. *Water* **10**, 748 (2018).
15. Mahé, G. & Paturel, J. E. 1896-2006 Sahelian annual rainfall variability and runoff increase of Sahelian Rivers. *C. R. Geosci.* **341**, 538–546 (2009).
16. Le Barbé, L., Lebel, T. & Tapsoba, D. Rainfall variability in West Africa during the years 1950-90. *J. Clim.* **15**, 187–202 (2002).
17. Tappan, G. G. et al. *Landscapes of West Africa: A Window on a Changing World* (CILSS, 2016).
18. Panthou, G. et al. Rainfall intensification in tropical semi-arid regions: the Sahelian case. *Environ. Res. Lett.* **13**, 064013 (2018).
19. Leblanc, M. J. et al. Land clearance and hydrological change in the Sahel: SW Niger. *Glob. Planet. Change* **61**, 135–150 (2008).
20. Favreau, G. et al. Land clearing, climate variability, and water resources increase in semiarid southwest Niger: a review. *Water Resour. Res.* **45**, W00A16 (2009).
21. Aich, V. et al. Climate or land use? Attribution of changes in river flooding in the Sahel Zone. *Water* **7**, 2796–2820 (2015).
22. Casse, C. et al. Model-based study of the role of rainfall and land use–land cover in the changes in the occurrence and intensity of Niger red floods in Niamey between 1953 and 2012. *Hydrol. Earth Syst. Sci.* **20**, 2841–2859 (2016).
23. Yonaba, R. et al. A dynamic land use/land cover input helps in picturing the Sahelian paradox: assessing variability and attribution of changes in surface runoff in a Sahelian watershed. *Sci. Total Env.* **757**, 143792 (2021).
24. Gardelle, J., Hiernaux, P., Kergoat, L. & Grippa, M. Less rain, more water in ponds: a remote sensing study of the dynamics of surface waters from 1950 to present in pastoral Sahel (Gourma region, Mali). *Hydrol. Earth Syst. Sci.* **14**, 309–324 (2010).
25. Gal, L. et al. The paradoxical evolution of runoff in the pastoral Sahel: analysis of the hydrological changes over the Agoufou watershed (Mali) using the KINEROS-2 model. *Hydrol. Earth Syst. Sci.* **21**, 4591–4613 (2017).
26. Kusserow, H. Desertification, resilience, and re-greening in the African Sahel; a matter of the observation period? *Earth Syst. Dyn.* **8**, 1141–1170 (2017).
27. Fensholt, R. et al. Greenness in semi-arid areas across the globe 1981–2007—an Earth Observing Satellite-based analysis of trends and drivers. *Remote Sens. Environ.* **121**, 144–158 (2012).
28. Dardel, C. et al. Re-greening Sahel : 30 years of remote sensing data and field observations (Mali, Niger). *Remote Sens. Environ.* **140**, 350–364 (2014).
29. Brandt, M. et al. Reduction of tree cover in West African woodlands and promotion in semi-arid farmlands. *Nat. Geosci.* **11**, 328–333 (2018).
30. Wang, L. et al. Dryland productivity under a changing climate. *Nat. Clim. Change* **12**, 981–994 (2022).
31. Fowler, K. et al. Hydrological shifts threaten water resources. *Water Resour. Res.* **58**, e2021WR031210 (2022).
32. Leduc, C., Favreau, G. & Schroeter, P. Long-term rise in a Sahelian water-table: the continental terminal in South-West Niger. *J. Hydrol.* **243**, 43–54 (2001).
33. Torou, B. M. et al. Constraints and opportunities for groundwater irrigation arising from hydrologic shifts in the Iullemmeden Basin, south-western Niger. *Water Int.* **38**, 465–479 (2013).
34. Di-Baldassarre, G. et al. Flood fatalities in Africa: from diagnosis to mitigation. *Geophys. Res. Lett.* **37**, 1–5 (2010).
35. Tazen, F. et al. Trends in flood events and their relationship to extreme rainfall in an urban area of Sahelian West Africa: the case study of Ouagadougou, Burkina Faso. *J. Flood Risk Manag.* **12**, e12507 (2019).
36. Tarchiani, V., Di Vecchia, A., Genesio, L. & Sorani, F., Monitoring drylands ecosystem dynamics for sustainable development policies: the Keita experience. In (eds C. Lee & T. Schaaf) *The Future of Drylands*, 395–407 (Springer Netherlands, 2008).
37. Sacande, M. & Muir, G. Restoring Sahelian landscapes with people and plants: insights from large-scale interventions. *Restor. Ecol.* **30**, e13656 (2022).
38. Maes, S. L. et al. Explore before you restore: incorporating complex systems thinking in ecosystem restoration. *J. Appl. Ecol.* **61**, 922–939 (2024).
39. IPCC, *AR6 Climate Change 2021: The Physical Science Basis* (IPCC, 2021).
40. Wendling, V. et al. Drought-induced regime shift and resilience of a Sahelian ecohydrosystem. *Environ. Res. Lett.* **14**, 105005 (2019).
41. Lebel, T. et al. AMMA-CATCH studies in the Sahelian region of West-Africa: an overview. *J. Hydrol.* **375**, 3–13 (2009).
42. Polcher, J., Parker, D. & Gaye, A. African monsoon multidisciplinary analysis: an integrated project for understanding of the West African climate system and its human dimension. *Atmos. Sci. Lett.* **12**, 1–1 (2011).
43. Galle, S. et al. AMMA-CATCH, a Critical Zone Observatory in West Africa monitoring a region in transition. *Vadose Zone J.* **17**, 1–24 (2018).
44. Chardon, D. et al. Stabilization of large drainage basins over geological time scales: Cenozoic West Africa, hot spot swell growth, and the Niger River. *Geochem. Geophys. Geosyst.* **17**, 1164–1181 (2016).
45. Lachassagne, P., Dewandel, B. & Wyns, R. Review: hydrogeology of weathered crystalline/hard-rock aquifers-guidelines for the operational survey and management of their groundwater resources. *Hydrogeol. J.* **29**, 2561–2594 (2021).
46. Bianchi, M., Palamakumbura, R. N., MacDonald, A. M. & Macdonald, D. M. J. Assessing regional variation in yield from weathered basement aquifers in West Africa and modelling their future groundwater development and sustainability. *Hydrogeol. J.* **31**, 257–274 (2023).
47. MacDonald, A. M. et al. Mapping groundwater recharge in Africa from ground observations and implications for water security. *Environ. Res. Lett.* **16**, 034012 (2021).
48. Villholth, K. G. Groundwater irrigation for smallholders in Sub-Saharan Africa - a synthesis of current knowledge to guide sustainable outcomes. *Water Int.* **38**, 369–391 (2013).
49. Shah, T., Namara, R. & Rajan, A. *Accelerating Irrigation Expansion in Sub-Saharan Africa* (World Bank, 2020).
50. Hiernaux, P. et al. Sahelian rangeland response to changes in rainfall over two decades in the Gourma region, Mali. *J. Hydrol.* **375**, 114–127 (2009).
51. Nkrumah, F. et al. Recent trends in the daily rainfall regime in Southern West Africa. *Atmosphere* **10**, 741 (2019).
52. Nguyen, C. C. *Dynamique, Structure et Production de la Végétation du Gourma (Sahel, Mali) en Relation avec les Sols, l'occupation des Sols et les Systèmes Hydriques : éTude de Télédétection à Haute et Moyenne Résolution*. PhD thesis (University of Toulouse 3, 2015).
53. Scheffer, M. & Carpenter, S. R. Catastrophic regime shifts in ecosystems: linking theory to observation. *Trends Ecol. Evol.* **18**, 648–656 (2003).
54. Mckee, T., Doesken, N. & Kleist, J. The relationship of drought frequency and duration to time scales. In *Proc. Eighth Conference on Applied Climatology* (AMS, 1993).

55. Berdugo, M. et al. Global ecosystem thresholds driven by aridity. *Science* **367**, 787–790 (2020).
56. Turnbull, L. et al. Understanding the role of ecohydrological feedbacks in ecosystem state change in drylands. *Ecohydrol* **5**, 174–183 (2012).
57. D'Odorico, P. et al. Global desertification: drivers and feedbacks. *Adv. Water Resour.* **51**, 326–344 (2013).
58. Mayor, A. G., Bautista, S., Rodriguez, F. & Kéfi, S. Connectivity-mediated ecohydrological feedbacks and regime shifts in drylands. *Ecosystems* **22**, 1497–1511 (2019).
59. Ludwig, J. A. & Tongway, D. J. Spatial organisation of landscapes and its function in semi-arid woodlands, Australia. *Landsc. Ecol.* **10**, 51–63 (1995).
60. Horton, R. E. The Role of infiltration in the hydrologic cycle. *Eos Trans. Am. Geophys. Union* **14**, 446–460 (1933).
61. Séguis, L. et al. Contrasted land-surface processes along the West African rainfall gradient. *Atmos. Sci. Lett.* **12**, 31–37 (2011).
62. Gbohoui, Y. P. et al. Impacts of climate and environmental changes on water resources: A multi-scale study based on Nakanbé nested watersheds in West African Sahel. *J. Hydrol.: Reg. Stud.* **35**, 100828 (2021).
63. Okin, G. S. et al. Do changes in connectivity explain desertification? *BioScience* **59**, 237–244 (2009).
64. Hoogmoed, W. B. & Stroosnijder, L. Crust formation on sandy soils in the Sahel I. Rainfall and infiltration. *Soil Tillage Res.* **4**, 5–23 (1984).
65. Valentin, C., Rajot, J. L. & Mitja, D. Responses of soil crusting, runoff and erosion to fallowing in the sub-humid and semi-arid regions of West Africa. *Agric., Ecosyst. Env.* **104**, 287–302 (2004).
66. Vandervaere, J. P. et al. Estimating hydraulic conductivity of crusted soils using disc infiltrometers and minitensiometers. *J. Hydrol.* **188–189**, 203–223 (1997).
67. Karambiri, H. et al. Assessing the impact of climate variability and climate change on runoff in West Africa: the case of Senegal and Nakambe River basins. *Atmos. Sci. Lett.* **12**, 109–115 (2011).
68. Trichon, V., Hiernaux, P., Walcker, R. & Mougin, E. The persistent decline of patterned woody vegetation: the tiger bush in the context of the regional Sahel greening trend. *Glob. Change Biol.* **24**, 2633–2648 (2018).
69. Mamadou, I. et al. Exorheism growth as an explanation of increasing flooding in the Sahel. *CATENA* **131**, 130–139 (2015).
70. Giertz, S., Diekkrueger, B. & Steup, G. Physically-based modelling of hydrological processes in a tropical headwater catchment (West Africa) - process representation and multi-criteria validation. *Hydrol. Earth Syst. Sci.* **10**, 829–847 (2006).
71. Hector, B. et al. Hydrological functioning of western African inland valleys explored with a critical zone model. *Hydrol. Earth Syst. Sci.* **22**, 5867–5888 (2018).
72. Mamadou, O. et al. Dynamics of water vapor and energy exchanges above two contrasting Sudanian climate ecosystems in Northern Benin (West Africa). *J. Geophys. Res. Atmos.* **121**, 11,269–11,286 (2016).
73. Nkiaka, E. et al. Quantifying the effects of climate and environmental changes on evapotranspiration variability in the Sahel. *J. Hydrol.* **642**, 131874 (2024).
74. Velluet, C. et al. Building a field- and model-based climatology of local water and energy cycles in the cultivated Sahel - annual budgets and seasonality. *Hydrol. Earth Syst. Sci.* **18**, 5001–5024 (2014).
75. Cuthbert, M. O. et al. Observed controls on resilience of groundwater to climate variability in sub-Saharan Africa. *Nature* **572**, 230–234 (2019).
76. Abdou Babaye, M. S. et al. Characterization of recharge mechanisms in a Precambrian basement aquifer in semi-arid south-west Niger. *Hydrogeol. J.* **27**, 475–491 (2019).
77. Kafando, M. B. et al. Influence of past climatic conditions on groundwater levels in basement aquifers of the Sahel. *Hydrogeol. J.* **33**, 531–551 (2025).
78. Vouillamoz, J. M., Lawson, F. M. A., Yalo, N. & Descloitres, M. Groundwater in hard rocks of Benin: Regional storage and buffer capacity in the face of change. *J. Hydrol.* **520**, 379–386 (2015).
79. Chagnaud, G., Panthou, G., Vischel, T. & Lebel, T. A synthetic view of rainfall intensification in the West African Sahel. *Environ. Res. Lett.* **17**, 044005 (2022).
80. Olsson, L. et al. Land degradation. In *Climate Change and Land: IPCC Special Report on Climate Change, Desertification, Land Degradation, Sustainable Land Management, Food Security, and Greenhouse Gas Fluxes in Terrestrial Ecosystems* (Cambridge University Press, 2019).
81. Peugeot, C. et al. Runoff generation processes: results and analysis of field data collected at the East Central Supersite of the HAPEX-Sahel experiment. *J. Hydrol.* **188-189**, 179–202 (1997).
82. Le Roux, E. et al. Hydrological regime shifts in Sahelian watersheds: an investigation with a simple dynamical model driven by annual precipitation. *Hydrol. Earth Syst. Sci.* **30**, 929–944 (2026).
83. Gardiya Weligamage, H. et al. Vegetation as a driver of shifts in rainfall-runoff relationship: Synthesising hydrological evidence with remote sensing. *J. Hydrol.* **648**, 132389 (2025).
84. Belete, M. D. Ecohydrological nature-based solution for climate resilience and biodiversity enhancement in water-limited ecosystem: perspectives and proof of concepts. *Ecohydrol. Hydrobiol.* **23**, 507–517 (2023).
85. Tramblay, Y. et al. ADHI: the African Database of Hydrometric Indices (1950-2018). *Earth Syst. Sci. Data* **13**, 1547–1560 (2021).
86. Chagnaud, G., Panthou, G., Vischel, T. & Lebel, T. Capturing and attributing the rainfall regime intensification in the West African Sahel with CMIP6 models. *J. Clim.* **36**, 1823–1843 (2023).
87. Sanogo, S. et al. Spatio-temporal characteristics of the recent rainfall recovery in West Africa. *Int. J. Climatol.* **35**, 4589–4605 (2015).
88. Biasutti, M. Rainfall trends in the African Sahel: characteristics, processes, and causes. *WIREs Clim. Change* **10**, e591 (2019).
89. Nicholson, S. E. Climatic and environmental change in Africa during the last two centuries. *Clim. Res.* **17**, 123–144 (2001).
90. Lebel, T. & Ali, A. Recent trends in the Central and Western Sahel rainfall regime (1990-2007). *J. Hydrol.* **375**, 52–64 (2009).
91. Singer, M. B. et al. Hourly potential evapotranspiration at 0.1° resolution for the global land surface from 1981-present. *Sci. Data* **8**, 224 (2021).
92. Muñoz-Sabater, J. et al. ERA5-Land: a state-of-the-art global reanalysis dataset for land applications. *Earth Syst. Sci. Data* **13**, 4349–4383 (2021).
93. R Core Team. *R: A Language and Environment for Statistical Computing* (R Foundation for Statistical Computing, 2021).
94. Boyer, J.F. et al. SIEREM: an environmental information system for water resources. In *Proc. Fifth FRIEND World Conference*, Vol 308, 19–25 (IAHS Publications, 2006).
95. Ekolu, J. et al. Long-term variability in hydrological droughts and floods in sub-Saharan Africa: new perspectives from a 65-year daily streamflow dataset. *J. Hydrol.* **613**, 128359 (2022).
96. Harris, I., Osborn, T. J., Jones, P. & Lister, D. Version 4 of the CRU TS monthly high-resolution gridded multivariate climate dataset. *Sci. Data* **7**, 109 (2020).
97. Mann, H. B. & Whitney, D. R. On a test of whether one of two random variables is stochastically larger than the other. *Ann. Math. Stat.* **18**, 50–60 (1947).

Acknowledgements

We thank the Directorate General of Water Resources (DGRE, Ministry of Environment, Water and Sanitation) of Burkina Faso, the Directorate

General of Water (DGEau, Ministry of Water and Mines) of the Republic of Benin, and the Niger Basin Authority for their help in accessing streamflow data. We also thank V. Dakos, S. Kuppel and C. Valentin for fruitful discussions. The 1950 topographic maps were digitised and processed by La Telescop (https://www.latelescop.fr), Montpellier, France. Funding: This study was funded by the French National Research Agency (ANR) under contract no. ANR-20-CE01-0014-01. WV and ELR received fellowship support through this contract.

Author contributions

C.Pe. and T.L. proposed the initial ideas and designed the research. C.Pe. secured the funding and coordinated the research. V.W., N.R., G.F. and F.B.D. curated and processed the runoff datasets. G.P. and T.V. processed the rain gauge datasets. A.C.B. processed the 1950 land cover statistics. C.Pe., V.W., E.L.R., G.P. and B.H. framed the paper's hypotheses. J.D., L.D., J.E., M.G., P.H., A.I.W., L.K., M.M.A., E.M., C.Pi., J.L.R. and J.P.V. were involved in conceptualising Sahelian land surface processes. J.M.C., B.H. and G.F. contributed to the understanding of the role of groundwater in hydrological changes. C.Pe. and V.W. drafted the manuscript and created the figures. All authors discussed the results and edited the manuscript.

Funding

This study was funded by the French National Research Agency (ANR) under contract no. ANR-20-CE01-0014-01. WV and ELR received fellowship support through this contract.

Competing interests

The authors declare no competing interests

Additional information

Supplementary information The online version contains supplementary material available at https://doi.org/10.1038/s41467-026-72648-6.

Correspondence and requests for materials should be addressed to Christophe Peugeot.

Peer review information *Nature Communications* thanks Raoul Collenteur, Kyle Compare, Scott Robeson, and the other anonymous reviewer for their contribution to the peer review of this work. A peer review file is available.